

MTGRBOOST: Boosting Large-scale Generative Recommendation Models in Meituan

Yuxiang Wang[†] Xiao Yan[†] Chi Ma[§] Mincong Huang[§] Xiaoguang Li[§] Lei Yu[§]
 Chuan Liu[§] Ruidong Han[§] He Jiang[§] Bin Yin[§] Shangyu Chen[§] Fei Jiang[§]
 Xiang Li[§] Wei Lin[§] Haowei Han[†] Bo Du[†] Jiawei Jiang[†]

[†] Wuhan University [§] Meituan

[†] {nai.yxwang,haowei.han,dubo,jiawei.jiang}@whu.edu.cn [†] yanxiaosunny@gmail.com

[§] {machi04,huangmincong,lixiaoguang12,yulei37,liuchuan11,hanruidong,jianghe06,
 yinbin05,chenshangyu03,jiangfei05,lixiang245,linwei31}@meituan.com

Abstract

Recommendation is crucial for both user experience and company revenue, and generative recommendation models (GRMs) are shown to produce quality recommendations recently. However, existing systems are limited by insufficient functionality support and inefficient implementations for training GRMs in industrial scenarios. As such, we introduce MTGRBoost as an efficient and scalable system for GRM training. Specifically, to handle the real-time insert/delete of sparse embedding entries, MTGRBoost employs dynamic hash tables to replace static tables. To improve efficiency, MTGRBoost conducts dynamic sequence balancing to address the computation load imbalances among GPUs and adopts embedding ID deduplication alongside automatic table merging to accelerate embedding lookup. MTGRBoost also incorporates implementation optimizations including checkpoint resuming, mixed precision training, gradient accumulation, and operator fusion. Extensive experiments show that MTGRBoost improves training throughput by $1.6\times - 2.4\times$ while achieving good scalability when running over 100 GPUs. MTGRBoost has been deployed for many applications in Meituan and is now handling hundreds of millions of requests on a daily basis.

1 Introduction

As a leading e-commerce platform for lifestyle services, Meituan spans multiple business verticals such as delivery, travel, and health. In 2024, we served over 770 million transacting users and processed more than 98 million orders at the daily peak. As shown in Figure 1, recommendation models [13, 25, 36, 45, 47] are at the core of our business by effectively filtering information and personalizing services for users. High-quality recommendations are crucial to sustain high customer retention rates, ensure merchant satisfaction, and enhance company revenue. Currently, our recommendation model incorporates terabytes of user behavioral data and item metadata for training on a daily basis and produces billions of predictions for various services.

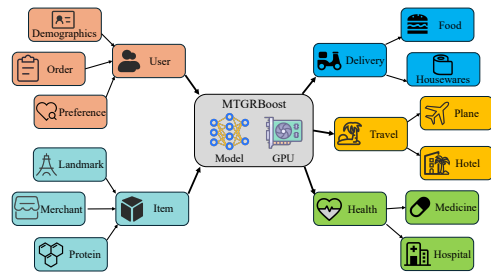


Figure 1: Applications of recommendation model in Meituan.

Following the advancements of generative language models [1, 26, 33, 34], generative recommendation models (GRMs) [4, 8, 11, 37, 42–44] have gained significant attention from both academia and industry. In particular, a GRM consists of two modules, i.e., *sparse embedding tables* that map discrete categorical features to continuous embedding vectors, and a *Transformer-based dense model* that predicts the next user action by modeling the action sequences of users. In contrast, earlier deep recommendation models (DRMs) [25, 36, 41, 47] utilize multilayer perceptrons to capture the interaction between user and each individual action. As shown in Figure 2, GRM achieves superior accuracy compared with DRM, primarily due to its ability to model the entire action sequence of each user with self-attention. However, GRM has greater computation complexity due to its attention mechanism, which scales quadratically with sequence length, while DRM scales only linearly. As such, to enjoy the good accuracy of GRMs and keep up with the high speed of training data generation, Meituan requires an efficient and scalable system for training GRMs.

Extensive researches have been conducted to optimize the execution of Transformer-based dense models [3, 9, 24, 28, 30]. For instance, FlashAttention [3] accelerates attention computation by materializing less intermediate results and hence reducing the accesses GPU global memory. Distributed training frameworks such as Megatron [30] and DeepSpeed [28] enhance scalability by using hybrid parallel training strategies

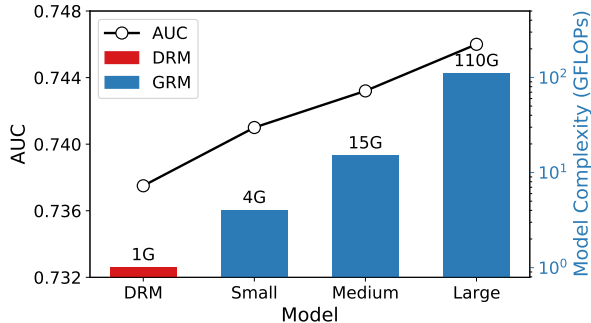


Figure 2: AUC (for accuracy, higher the better) and model complexity for DRM and GRM. An accuracy improvement of even 0.1% is crucial for practical recommendation.

that combine data, model, and pipeline parallelism. These developments motivate a migration from TensorFlow [31] to PyTorch [15] for industrial recommendation systems. In particular, TorchRec [10] is the state-of-the-art PyTorch-based system for recommendation model training, and we develop MTGRBoost based on it by integrating efficient attention computation kernels.

However, we identify two fundamental inefficiencies in TorchRec when handling the sparse embedding tables of GRMs. ❶ TorchRec’s static embedding tables can not process dynamic embedding entries and table capacity expansion. Specifically, additional embeddings cannot be allocated to new users and items (e.g., merchants updating menus) at real-time from fixed-size static tables. Although some default embeddings may be used in this case, model accuracy will be degraded. Static tables inherently lack dynamic expansion capabilities. Thus, static tables typically require pre-allocation of capacity exceeding actual requirements to prevent ID overflow, inevitably leading to inefficient memory utilization. ❷ For embedding lookup, TorchRec can fetch the same embedding entry multiple times due to duplicate feature IDs in sequences, which causes a long communication time and wastes network bandwidth. Moreover, TorchRec requires labor-intensive manual configuration to merge the embedding tables, which is a common and effective operation to accelerate training. The two limitations severely constrain GRM’s practical deployment and compromise training efficiency.

To tackle the challenges, MTGRBoost features a hash-based dynamic embedding table and two associated optimizations, i.e., automatic table merging and lookup deduplication. The hash-based embedding table eliminates fixed-capacity constraints by decoupling the storage of keys (i.e., embedding index) and values (i.e., embedding vector) and uses hash functions to map arbitrary feature IDs to embedding index. We tailor the capacity expansion process by maintaining two value allocations and only doubling the key storage. The insight is that the network communication for migrating the keys is significantly lower than moving the high-dimensional embedding vectors as for the static tables. Moreover, we adopt

two-stage ID unique operation to reduce redundant IDs before and after ID communication to avoid repetitive embedding transfers among the devices. We also design a feature configuration interface to implement automatic table merging, which can reduce the number of embedding lookup operators and thus speed up the process.

Besides the sparse embeddings, MTGRBoost incorporates a suite of additional optimizations to implement an efficient GRM training system. We observe that variable-length sequences cause significant load imbalances among the GPUs. Since retaining complete sequences is crucial for accuracy, we cannot truncate or pad sequences for load balancing as done for LLMs. Instead, we propose a light-weight dynamic sequence balancing technique, which dynamically adjusts the batch sizes for GPUs such that the GPUs have similar workload. Moreover, MTGRBoost supports checkpoint resumption, mixed-precision training, gradient accumulation, and operator fusion. In particular, MTGRBoost allows saving and loading checkpoints using different numbers of GPUs, uses different precisions for the dense model, hot embeddings, and cold embeddings to reduce computation, conducts efficient sparse gradient accumulation through sparse aggregation, and accelerates forward computation by fusing multiple kernels in the attention modules.

We evaluate MTGRBoost and its designs using 300 million real user sequences generated during a week at Meituan. Scalability experiments show that MTGRBoost achieves close to linear speedup in training throughput when using more GPUs. Compared with TorchRec, MTGRBoost reduces the training time by $2.44\times$. Ablation experiments show that our designs are effective. In particular, dynamic sequence balancing achieves near-optimal load balance and improves system throughput by $1.75\times$ compared to the baseline. Moreover, automatic table merging and lookup de-duplication significantly reduce network communication, yielding an improvement of 53% in throughput.

To summarize, we make the following contributions.

- We present MTGRBoost as an efficient and scalable system for training generative recommendation models (GRMs) at Meituan in real production environment.
- We observe that existing systems are inefficient when handling the sparse embeddings of GRMs. As such, we propose techniques including dynamic table to adapt changing features, automatic table merging to fuse operators, and lookup de-duplication to avoid repetitive communication.
- We build MTGRBoost as a complete and efficient system for GRM training with optimizations including load balancing, flexible checkpoint resumption, mixed-precision computation, gradient accumulation, and kernel fusion.
- We conduct extensive experiments on real data from production to evaluate MTGRBoost. The results show that MTGRBoost is efficient and scalable, and our designs are effective in improving system efficiency.

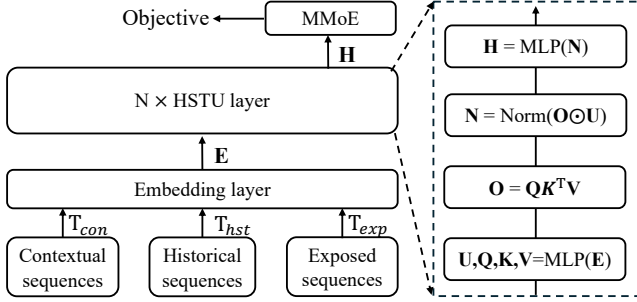


Figure 3: Model architecture of Meituan’s GRM.

2 GRM in Meituan

Model Architecture. Figure 3 illustrates the model architecture of the generative recommendation model (GRM) in Meituan, which consists of four core components: input sequence, embedding layer, hierarchical sequential transduction units (HSTU) layer, and multi-gate mixture-of-experts (MMoE) layer. In particular, the input sequence $\mathbf{T} = [T_{con}, T_{hst}, T_{exp}]$ includes contextual sequences (i.e., user features), historical sequences (e.g., click and purchase actions), and exposed sequences (i.e., real-time actions). Since the deep model cannot directly process discrete category data, the embedding layer ϕ_{emb} is used to convert the feature IDs into continuous embedding vectors $\mathbf{E} = \phi_{emb}(\mathbf{T}) \in \mathbb{R}^{F \times d}$, where F and d denote the number of features and embedding dimensions, respectively.

Subsequently, we employ multiple HSTU layers – an attention-based Transformer architecture – to learn user sequence embeddings through user and item interactions. As shown in Figure 3, each HSTU is equipped with four attention-based sub-layers for user feature extraction \mathbf{U} , item feature extraction \mathbf{O} , and feature interaction \mathbf{H} . We formulate the calculation process as follows:

$$\mathbf{U}, \mathbf{Q}, \mathbf{K}, \mathbf{V} = \text{Split}(\phi_1(\text{MLP}(\mathbf{E}))), \quad (1)$$

$$\mathbf{O} = \phi_2(\mathbf{Q}\mathbf{K}^T)\mathbf{V}, \quad (2)$$

$$\mathbf{H} = \text{MLP}(\text{Norm}(\mathbf{O} \odot \mathbf{U})), \quad (3)$$

where ϕ_1 and ϕ_2 are the SiLU activation function. MMoE directs embeddings \mathbf{H} from the HSTU layer to multiple expert models. Each expert model is equipped with a gating network that learns the model’s weights. We finally aggregate the output embeddings of the top- k expert models. That is:

$$y = \sum_{i=1}^k g_i(\mathbf{H}) \cdot \text{Expert}_i(\mathbf{H}). \quad (4)$$

We use cross entropy loss to optimize click-through rate and conversion rate.

Different from GRM and DRM. Our model builds upon GR [44] by introducing a novel prediction head enhanced

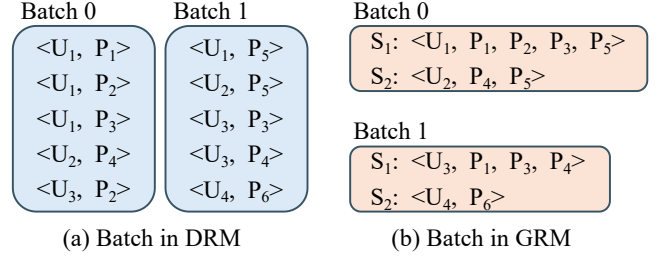


Figure 4: Batch structure of DRM and GRM. “ U ” denotes users, “ P ” denotes products. DRM and GRM use a pairwise and sequence-wise batch construction method, respectively.

through MMoE. This design replaces GR’s MLP with MMoE, which employs task-specific gate networks to dynamically balance multiple objectives, improving accuracy in multi-task scenarios. Compared to MLP’s parameter-intensive tuning, MMoE reduces computational overhead by selectively activating only the top- k expert outputs. Additionally, our MTGRBoost diverges from DRM in batch construction. As illustrated in Figure 4, DRM’s pairwise batches contain redundant user computations (e.g., “User 1” features are processed twice). In contrast, MTGRBoost employs a sequence-wise approach that consolidates multiple user interactions into a single sample, which ensures each user feature is computed once. Notably, user features contain orders of magnitude more tokens than item features (e.g., 10,000 vs. 100), enabling MTGRBoost to significantly accelerate training and improve scalability.

3 MTGRBoost System Overview

MTGRBoost facilitates the distributed training of GRMs across multiple devices. For parallelism, we follow the TorchRec’s design and employ a hybrid strategy: model parallelism for sparse models and data parallelism for dense models. This combined approach is informed by two considerations. Firstly, data parallelism is impractical for the large embedding table, as no single device can accommodate the entire table. Secondly, the dense models are relatively small, which renders data parallelism more suitable. MTGRBoost is trained end-to-end with synchronous execution, ensuring model quality and accuracy.

Workflow. We provide the detailed explanation as follow.

- **Data I/O.** As shown in Figure 5 (1), the training data is stored in partitioned Hive tables on HDFS, which utilizes a columnar storage format to optimize access speed and storage efficiency. Each column in the Hive table represents a feature. To maximize I/O throughput, the Hive tables are partitioned into smaller shards distributed across devices, which read data in parallel from their assigned shards. Additionally, we prefetch multiple next batches and overlap

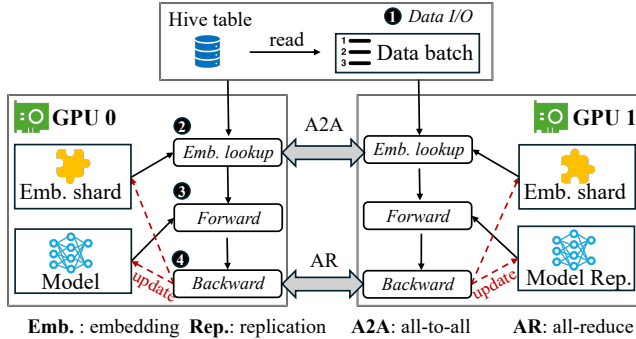


Figure 5: The workflow of MTGRBoost for GRM training.

their loading with the computation of the current batch, thereby masking I/O latency.

- **Embedding Lookup.** As shown in Figure 5 (2), the embedding lookup process employs All-to-all communication for cross-device embedding exchange. In particular, this process involves two data exchanges: First, devices transmit feature IDs requiring queries and receive corresponding IDs from peer devices through All-to-all communication. Subsequently, another All-to-all operation facilitates the exchange of retrieved embeddings between devices.
- **Forward Computation.** The dense models within MTGRBoost, including HSTU and MMoE, have significantly fewer parameters compared to sparse model (i.e., embedding tables). As depicted in Figure 5 (3), data parallelism prepares a replication of the dense model for each device during forward propagation. Model parameters across all devices are consistently initialized by setting the same random seed. MTGRBoost partitions the total sequence batch into smaller micro-batches distributed to various devices, then performs forward computation in parallel.
- **Backward Update.** Figure 5 (4) illustrates the heterogeneous parameter update adopted by MTGRBoost in the hybrid parallel architecture. Sparse embedding tables aggregate shard gradients through model parallelism, where each device updates its locally stored embedding shards via All-to-all communication. Dense parameters (e.g., HSTU) employ All-Reduce communication for gradient synchronization before parameter update.

Pipeline. To further enhance training efficiency, we maximize parallelism through pipeline technology using three streams: *copy*, *dispatch*, and *compute*. Specifically, the copy stream loads sequences from CPU to GPU, the dispatch stream performs table lookups based on IDs, and the compute stream handles forward computation and backward updates. For instance, while the compute stream executes forward and backward passes for batch T , the copy stream concurrently loads batch $T + 1$ to mask I/O latency. Upon completing backward

updates for batch T , the dispatch stream immediately initiates table lookups and communication for batch $T + 1$.

4 Efficient Processing for Sparse Embeddings

4.1 Dynamic Embedding Table

In Meituan’s production environment, the recommendation system must dynamically adjust recommendations based on real-time user interactions. However, TorchRec cannot handle dynamic IDs due to its reliance on fixed-capacity static embedding tables. Static tables typically use default embeddings to provide embeddings for feature IDs that exceed the capacity, but it leads to model accuracy degradation. Furthermore, static table necessitates over-provisioning of initial capacity to anticipate potential expansion requirements, which results in inefficient memory utilization. These limitations motivated MTGRBoost’s implementation of dynamic embedding tables.

Storage Layout. MTGRBoost employs a decoupled architecture for hash table, which separates key and value storage into distinct structures. As shown in Figure 6 (a), the *key structure* maintains a lightweight mapping table containing keys and corresponding pointers to embedding vectors, while the *embedding structure* stores both the embedding vectors and auxiliary metadata (e.g., counters and timestamps) required for eviction policies like Least Recently Used and Least Frequently Used. This dual-structure design achieves two critical objectives: (1) enabling dynamic capacity expansion through replication of only the compact key structure rather than huge embedding data, and (2) optimizing key scanning efficiency by storing keys in compact memory layouts while accommodating potentially sparse key distributions.

Furthermore, we implement chunk-based allocation for the embedding structure. This design provides two benefits: first, it reduces memory fragmentation through bulk allocation of larger chunks rather than frequent small allocations, while enabling efficient single-operation deallocation; second, it enhances cache locality through sequential memory access patterns, thereby improving hash table access efficiency.

Handling Hash Function and Collisions. MTGRBoost selects MurmurHash3 [2] as the hash function to determine where the embedding data is stored. MurmurHash3 processes input ID in 4-byte blocks through mixing operations (e.g., constant multiplication, bit rotation, XOR merging) to maximize entropy and ensure avalanche effects from single-bit changes. The multi-stage mixing generates uniformly distributed hash values through iterative nonlinear transformations.

Hash collisions occur when different keys are mapped to the same index position by the hash function. Techniques such as chaining and open addressing are typically employed. MTGRBoost chooses open addressing to resolve collisions due to its memory efficiency advantages over chaining. However, existing probing techniques exhibit vulnerability to cluster-

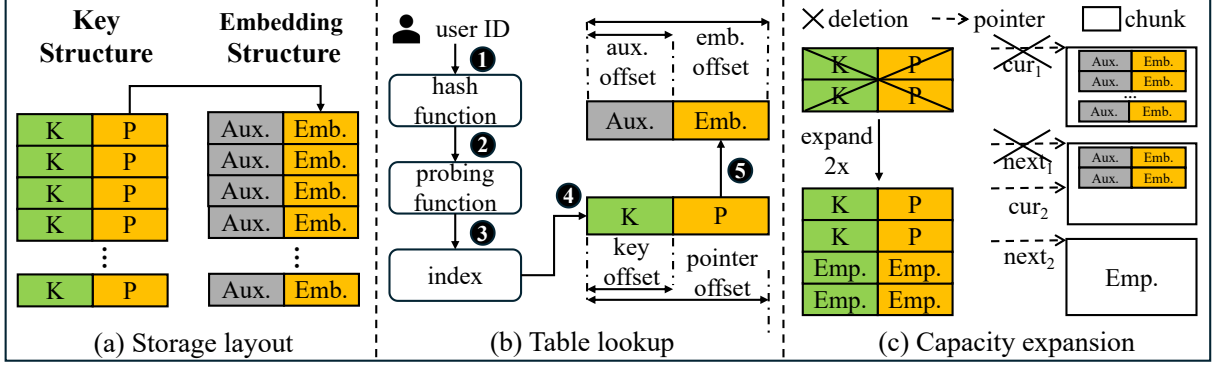


Figure 6: Dynamic embedding table in MTGRBoost. (a) *Storage layout*. We design a decoupled key-value storage architecture, where keys are stored in the Key Structure and values reside in a dedicated Embedding Structure. (b) *Table lookup*. For a given ID, we employ hash and probing functions to identify its index, and then retrieve the embedding’s memory address using an offset-based mechanism. (c) *Capacity expansion*. We prioritize key structure expansion and initiate embedding structure expansion only when the current memory chunk reaches capacity.

ing behavior under high load factors. To address this issues, we propose a novel grouped parallel probing technique. This approach begins by ensuring that the base step size S is an odd number through a bitwise OR operation with 1, thereby guaranteeing that all positions in the table can be accessed during probing. Next, we associate the step size with the key to prevent clustering that results from overlapping probing sequences of different keys. Finally, we multiply the step size by the thread group number, enabling distinct thread groups to probe different regions of the table. Formally, this technique is expressed as follows:

$$S = (k\%(M/\text{threads} - 1) + 1 | 1) * \text{threads}, \quad (5)$$

where k refers to the key’s value, M represents the hash table size, threads indicates the number of thread groups, and $|$ denotes the bitwise OR operation. Grouped parallel probing leverages the highly parallel capabilities of GPUs, ensuring a uniform distribution of the probing sequence. Moreover, we use coprime conditions to prove that our grouped parallel probing technique can traverse all slots in the hash table. The proof is provided in Appendix A.

Theorem 1 For a hash table of size $M = 2^n$ and an odd probing step S , the probe sequence $\{h_i\}_{i=0}^{M-1}$, $h_i = (h_0 + iS)\%M$ covers all M distinct slots if and only if S is odd. Formally:

$$\forall i, j \in [0, M - 1], i \neq j \Rightarrow h_i \neq h_j. \quad (6)$$

Table Lookup. With the hash function and probing method in place, we can now implement dynamic table lookup effectively. As shown in Figure 6 (b), a hash value is computed for a given user ID, and probing identifies the index corresponding to this ID within the hash table (steps 1-3). Using the starting address of the key structure in memory, along with

the index and pointer offset, we determine the embedding pointer p for the user ID (step 4), formally defined as follows:

$$p = st_add + index * row_offset + pointer_offset, \quad (7)$$

where st_add denotes the start address of key structure, and $row_offset = key_offset + pointer_offset$. Finally, we use this pointer, along with the embedding offset in the embedding structure, to extract the embedding vector (step 5). Unlike static tables, which cannot handle input data ranges exceeding their size, our dynamic table can accept changeable input value. Consequently, the dynamic table effectively addresses the limitation of static tables on managing dynamic IDs.

Capacity Expansion. MTGRBoost initiates hash table expansion when slot occupancy reaches critical levels (typically at load factors >0.75). As depicted in Figure 6 (c), capacity follows a power-of-two progression, doubling iteratively until meeting system requirements. The migration process transfers the keys and pointers from the original key structure to the expanded version and then deallocating the legacy memory. Crucially, our design prioritize expanding the key structure while maintaining the chunk (i.e., embedding structure) capacity, thus optimizing expansion efficiency by avoiding bulk embedding data transfers. MTGRBoost maintains two chunks – a current chunk and a next chunk – to address embedding structure expansion requirements. Specifically, when the current chunk’s remaining capacity becomes insufficient to accommodate new embeddings, we store them in the next chunk. Concurrently, we retire the filled chunk and allocate a new chunk as the next chunk to preserve the dual-chunk configuration. This pre-allocation mechanism ensures immediate storage availability for new embeddings during expansion.

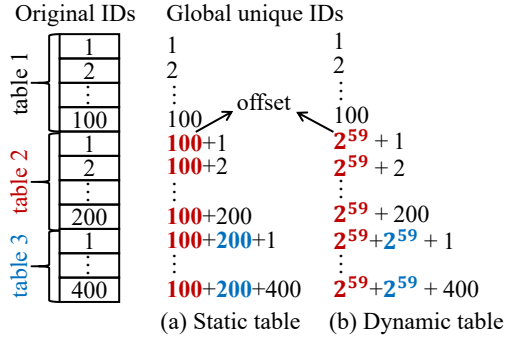


Figure 7: An example of offsets in static table and hash table.

4.2 Embedding Table Merging

Industrial recommendation systems usually merge multiple separate embedding tables into a larger and unified table. Merging tables offers two key advantages. First, the merged embedding table is stored as a contiguous memory block, which avoids memory fragmentation issues. Second, the merged table significantly enhances lookup efficiency, as multiple table lookup operations are fused into a single operation. However, we observe critical limitations in TorchRec’s table merging implementations. The merging process requires developers to manually configure each embedding table individually, which becomes labor-intensive for massive tables.

Automated Merging Table. To address the above issue, we propose an automated table merging framework. We design a unified feature configuration interface, `FeatureConfig`, which enables automated merging by defining parameters for each feature (e.g., *feature name*, *embedding dimensions*, and *lookup tables*). `MTGRBoost` then generates merging strategies, such as combining tables with identical embedding dimensions. To support dynamic embedding table merging, we design `HashTableCollection`, which generates a collection of hash tables using feature configurations and performs pooling computations as needed. Finally, `MTGRBoost` retrieves embeddings via sequence IDs, with cross-table lookups managed through predefined lookup tables. Developers need only specify required features and `MTGRBoost` automatically registers features and executes table merging without manual intervention in implementation details.

Previous Solution. Merging table may lead to numerical overlap in the ID space of different tables. For example, both user ID and item ID might have the same ID value in the whole merged table. To address this issue, recommendation systems typically employ a row-wise offset mechanism. As shown in Figure 7 (a), a unique row offset value is assigned to each embedding table (i.e., offset 100 for table 2), calculated by summing the number of rows from all preceding embedding tables. This offset is then added to the original ID to generate a globally unique ID, which is used to retrieve the

corresponding embedding from the merged table.

Our Solution. The dynamic table merging also encounters the issue of ID numerical overlap. However, because the number of rows in dynamic tables cannot be accessible in advance and thus fixed row offsets cannot be directly applied. To address this issue, we allocate the largest possible offset for each dynamic table to prevent ID overflow. We still use row offsets to calculate globally unique IDs, however, these offsets are dynamically calculated based on the number of feature tables. Specifically, we use bitwise operations to combine the original ID with a feature table identifier to create a globally unique ID. We begin by computing the number of bits needed for encoding feature table indices as $k = \lceil \log_2(m+1) \rceil$, using the high k bits of the 64-bit integer space as feature identifier bits. We ensure the offset is a positive integer by setting the highest bit to 0, while the remaining $(64-1-k)$ bits are used to calculate the maximum number of row in the hash table. As illustrated in Figure 7 (b), we use 2 identifier bits to distinguish between three tables (since $\lceil \log_2(3+1) \rceil = 2$), while calculating the maximum row capacity of hash table as 2^{61} through utilization of the remaining 61 bits $(64-1-2)$. Consequently, the offset values for “Table 2” and “Table 3” are configured as 2^{59} and 2^{60} , respectively, derived through successive halving of the maximum row capacity. Formally, the calculation formula for the ID x in the i -th feature table is as follows:

$$\text{ID} = (i \ll (63 - k)) | x, \quad (8)$$

where \ll denotes shift left operation, $|$ is bitwise OR.

4.3 Embedding Table Lookup Acceleration

For industrial recommendation systems, embedding tables are typically divided into shards distributed across multiple devices. Exchanging embedding vectors across devices requires two all-to-all collective communications for each table lookup: ID communication and embedding communication. ID communication involves exchanging feature IDs to be queried, while embedding communication entails exchanging the queried embeddings. However, a sequence batch may contain numerous duplicate feature IDs, and limited bandwidth can render ID communication and embedding communication as performance bottlenecks. Additionally, duplicate feature IDs result in redundant reads of the same embedding vector, significantly increasing memory access pressure.

Two-stage ID Deduplication. To address the issues mentioned, Figure 8 illustrates a two-stage ID deduplication process aimed at reducing communication latency and lookup frequency. In the first stage, latency is decreased in two critical areas: feature ID communication and embedding communication. Devices within nodes deduplicate feature IDs before exchanging them, resulting in reduced ID communication latency. More importantly, deduplication significantly alleviates embedding communication latency. If IDs are redundant,

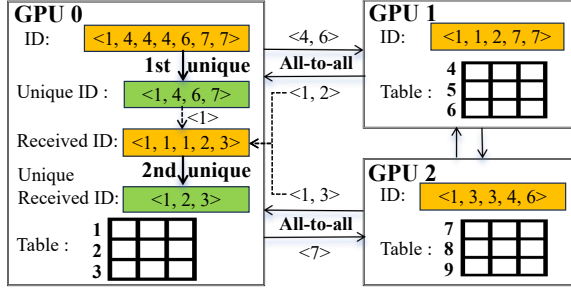


Figure 8: A running example of two-stage ID deduplication. We only visualize the ID deduplication process on GPU 0 and omit the embedding communication.

devices will transmit multiple duplicate embeddings, as they must return the corresponding embedding vectors based on the received feature IDs. Despite optimization efforts in the first stage, the all-to-all ID exchange inherently reintroduces duplicate IDs across devices due to distributed communication patterns. The second deduplication stage removes these newly generated duplicates, thereby minimizing the frequency of table lookups. Notably, the primary objective of the two-stage ID uniqueness operation is to reduce embedding communication latency, as ID communication has a relatively minor impact and hash table lookups are inherently efficient.

5 Additional Optimizations

5.1 Sequence Balancing

User sequences naturally exhibit a long-tail distribution: a small subset of highly active users generate exceptionally long sequences, while the majority produce relatively short ones. Previous deep recommendation models (DRMs) are constrained by architectural limitations that enforce sequence truncation and padding for length alignment. In contrast, generative recommendation models (GRMs) preserve complete user sequences, thereby achieving superior accuracy. This advantage arises because truncation risks removing semantically critical tokens (i.e., an item in the sequence), even when separated by many intermediate interactions. For example, a user’s early phone purchase history may influence subsequent accessory recommendations despite temporal distance. Furthermore, truncation alters the fundamental semantics of sequential dependencies.

Initial Design. FlashAttention [3] processes sequences by dividing them into chunks, where each chunk independently computes local attention. The final results are iteratively merged to cover the full sequence. This chunk-based design inherently supports variable-length sequences, motivating our initial approach of directly computing complete user sequences with flash attention. We then randomly sample a fixed number of sequences to form training batches and

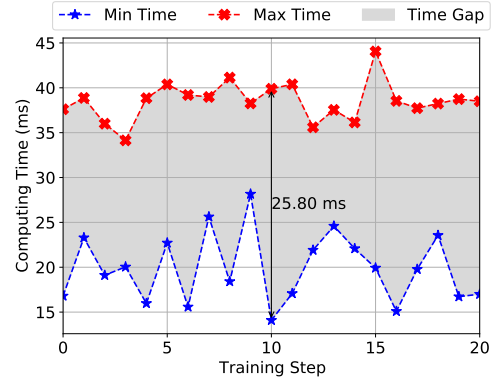


Figure 9: The visualization of imbalanced computational load. We train the MTGRBoost on 8 GPUs and report the maximum and minimum GPU computation times across steps 0–20. The shaded region indicates GPU idle time.

Algorithm 1: Dynamic Sequence Batching

Input: Target token count N , input chunks \mathcal{C}

$Q \leftarrow \emptyset, C_i \in \mathcal{C}, i = 0$

while $C_i \neq \emptyset$ **do**

if $\text{sum}(Q) < N$ **then**

$Q \leftarrow \text{add all sequence in } C_i$

$i++$

$S \leftarrow \text{cumulative sum of sequence token count in } Q$

$k \leftarrow \text{binary search in } S \text{ for closest value to } N$

if $k < \text{len}(Q)$ **then**

$\mathcal{B} \leftarrow \text{pop}(Q[:k])$

yield \mathcal{B}

Output: Balanced batch \mathcal{B}

distribute them across devices. However, this straightforward batching approach resulted in significant efficiency challenges. Figure 9 illustrates the range of GPU computation times per training step. The shaded region in the figure reveals prolonged synchronization delays (up to 25.8 ms) across devices, resulting in resource underutilization and reduced training efficiency. The primary cause is the unequal distribution of sequence length: within a single training step, devices process token quantities differing by as much as 40,000. To mitigate this issue, we propose a novel dynamic sequence batching method to balance computational loads across devices.

Dynamic Sequence Batching Algorithm 1 illustrates MTGRBoost’s dynamic sequence batching mechanism, where each GPU maintains a buffer Q for storing sequence samples retrieved from hive table chunks $C_i \in \mathcal{C}$. We define target token count N as the product of average sequence length (i.e., 600) and batch size. The system first computes token counts per sample in the sequence buffer and calculates cumulative sums S . A binary search algorithm then identifies the optimal partition point k where the cumulative sum most closely ap-

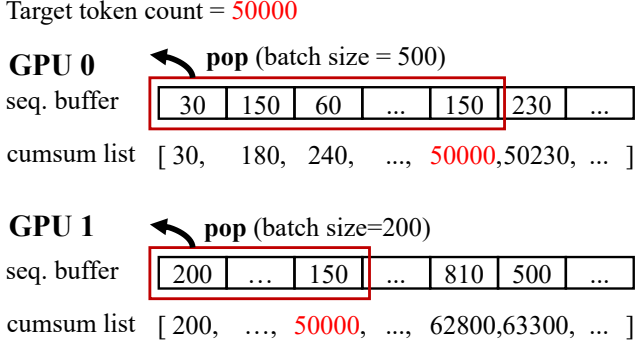


Figure 10: Running example of dynamic sequence batching. The number indicates the number of tokens in a sample.

proaches the target token count. We finally obtain a balanced batch \mathcal{B} by outputting the first k sequences in the buffer. When total buffer tokens fall below the target, remaining samples merge into subsequent buffer. This process iterates until all have table chunk samples are consumed.

In data parallelism, gradients are typically averaged using All-Reduce operations. However, with dynamic sequence batching, directly averaging gradients may introduce biases, as each device computes gradients based on a varying number of samples. To address this issue, we implement All-to-all communication to synchronize batch sizes across devices, followed by performing a weighted average of gradients proportional to their respective batch sizes. This mechanism ensures numerical correctness in both loss computation and gradient update processes.

Discussions. We observe two critical advantages of dynamic sequence batching in distributed training systems. First, device load balancing through constraining token counts. Second, optimized hardware utilization via dynamic batch sizes. As shown in Figure 10, GPU 0 requires 500 batches to reach the threshold while GPU 1 achieves it with 200 batches. Fixed size strategy requires conservative batch size configurations to prevent out-of-memory risks from clusters of extremely long sequences. In contrast, dynamic batching maximizes device memory utilization by loading batches near device memory limits. While more complex load balancing methods exist, including sequence packing based on length distributions [17, 19] or dynamic programming-based parallelism strategies [20], we ultimately exclude these methods from our MTGRBoost. This selection stems from the empirical observation that our lightweight dynamic sequence balancing achieves near-optimal workload balancing under current training conditions, rendering additional complexity unnecessary.

5.2 Implementations

Checkpoint Resuming. The core objective of checkpoint is to achieve persistent model preservation during training,

enabling rapid recovery to previous training states. MTGRBoost not only supports conventional checkpoint resuming but also facilitates preservation and loading in dynamic distributed environments (e.g., saving on 8 GPUs but loading on 16 GPUs). Existing systems address this challenge by saving model parameters from all devices in a single checkpoint, then redistributing parameters based on new device quantities during loading. However, this approach suffers from a critical flaw: each device must scan the entire checkpoint, resulting in redundant read operations. In contrast, MTGRBoost implements a novel approach where each device independently preserves its own checkpoint. During loading, new devices locate required checkpoint files through modulo operations. For instance, when loading checkpoints saved from 8 GPUs onto 16 GPUs, both GPU 0 and GPU 8 load parameters from the checkpoint saved on the original GPU 0. This design is grounded in the insight that distributed cluster scaling typically follows powers of two.

Mixed Precision Training. During training, we reduce computational resource consumption by converting dense models from FP32 to FP16 precision. For sparse embeddings, we dynamically partition hot feature sets based on access frequency. Specifically, for high-frequency accessed feature embeddings, we preserve embedding vectors in FP32 format to avoid quantization accumulation errors caused by frequent gradient updates. Conversely, low-frequency features employ FP16 storage and computation, significantly reducing memory footprint while accelerating table lookup operations.

Gradient Accumulation. MTGRBoost enhances training stability by accumulating gradients across multiple training batches to mitigate large gradient variances caused by small batch sizes. For sparse embedding parameters, we first record activated embedding IDs and their corresponding gradient values within each batch. These gradients from identical IDs across multiple batches are accumulated and then updated collectively. Furthermore, we avoid full parameter updates for sparse embeddings, instead selectively updating only activated parts. This design simultaneously reduces memory waste and improves update efficiency. For smaller dense models, we also implement gradient accumulation followed by full parameter updates.

Operator Fusion. Inspired by Flash Attention, we implement customized operator fusion for the critical HSTU module in forward computation. Specifically, we partition the U, Q, K, and V matrices in Figure 3 into tiles and process them sequentially in SRAM. Crucially, we use casual mask vectors to reduce unnecessary calculations by dynamically determining token skipping.

Table 1: Model hyperparameters in GRM. **Complexity** denotes computational complexity, and the unit is FLOPs.

	Complexity	# Emb. dim.	# HSTU block	# HSTU head
Small	4G	512	3	2
Large	110G	1024	22	4

6 Experimental Evaluation

6.1 Experiment Settings

Model Setup. For GRM’s dense model, we scale model architecture based on *computational complexity*, resulting in GRM 4G and GRM 110G variants, where “G” corresponds to Giga Floating-Point Operations (GFLOPs) required per forward pass. For sparse models, we use the *embedding dimension factor* to expand the embedding tables, including 1D, 8D, and 64D configurations. The baseline 1D configuration chooses the widely adopted embedding dimensions [25, 36, 41], typically ranging from 32 to 128 (with variations across different features). Accordingly, 64D represents a $64\times$ expansion of all embedding table dimensions relative to this 1D baseline. We adjust the embedding dimension factor in experiments including time decomposition, lookup deduplication, dynamic table, and scalability due to these experiments are sensitive to embedding dimension, and keep a default value of 1 in other experiments. The detailed model hyperparameters are provided in Table 1.

Baselines. We compare MTGRBoost with TorchRec, the state-of-the-art GRM training framework proposed by Meta [10]. Actually, our initial design is developed based on TorchRec, and we further implement MTGRBoost with the proposed optimizations. We conduct experimental comparisons against TorchRec regarding both model accuracy and efficiency. In the ablation experiments, we investigate the effects of our designs in MTGRBoost. We exclude alternative baselines as TorchRec is the only PyTorch-native training framework specifically optimized for PyTorch-based GRMs. Although other training systems such as TensorFlow are widely used in the industry, their framework currently cannot support GRM training.

Dataset and Implementation. We conduct experiments on 90 days of user logs from Meituan, with daily log data exceeding 400 million sequences. The average sequence length is 600, reaching a maximum length of 3,000. All models are trained from scratch using the same data. To optimize sparse and dense features, we employ the Adam [16] optimizer.

Environment. Our experiments are conducted on a training node equipped with 8 GPUs by default. For scaling experiments, the cluster configuration extends to a maximum of 16 GPU nodes, each containing 8 GPUs. All GPUs are NVIDIA

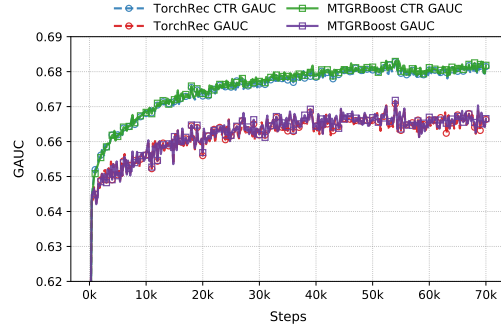


Figure 11: The GAUC results of CTR and CTCVR on GRM 4G 1D for TorchRec and MTGRBoost, respectively.

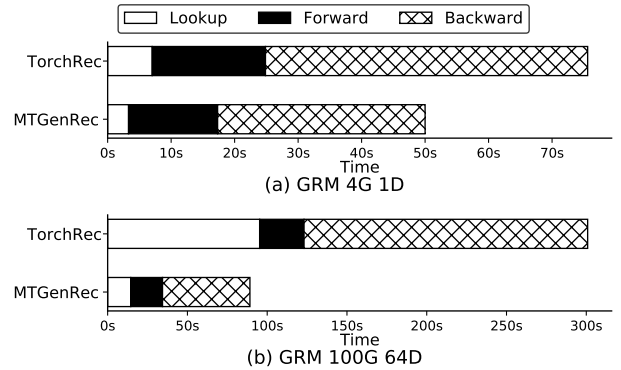


Figure 12: Time decomposition for GRM 4G 1D and GRM 100G 64D in TorchRec and MTGRBoost, respectively.

A100 SXM4 models with 80GB of memory. GPUs within a node are interconnected via NVLink with a bandwidth of 600 GB/s, while nodes are connected using Infini-Band interconnects with a bandwidth of 200 GB/s.

Evaluation Metrics. We use *Group AUC* to evaluate the accuracy of the model on CTR and CTCVR tasks and *system throughput* to evaluate the training efficiency. GAUC calculates the AUC metric by grouping at the user level, which can better reflect the actual performance of the recommendation model compared to conventional global AUC.

6.2 Comparisons to Baselines

Accuracy. Figure 11 presents the CTR and CTCVR GAUC results obtained from training a generative recommendation model using MTGRBoost and TorchRec. The GRM models in two systems exhibit rapid GAUC growth during the initial 40,000 training steps, followed by gradual improvement over the subsequent 30,000 steps before stabilizing. This progression demonstrates that both MTGRBoost and TorchRec ensures both model correctness and training stability.

Time Decomposition. Figure 12 presents the time decomposition of GRM 4G 1D and GRM 50G 64D across 100

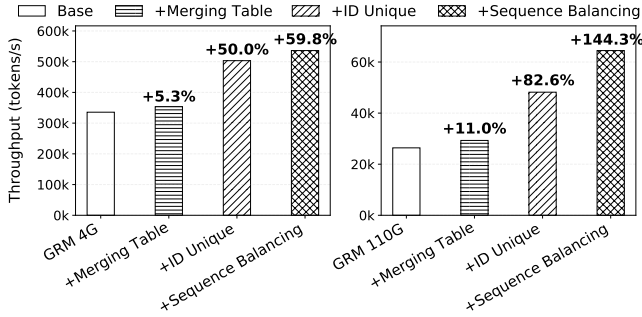


Figure 13: Ablation study for GRM 4G 1D and GRM 110G 1D in MTGRBoost. Compared with the baseline, MTGRBoost achieves a $1.60\times$ to $2.44\times$ throughput improvement.

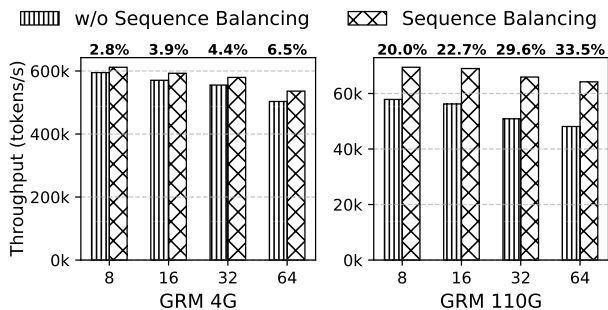


Figure 14: Throughput comparison for disabling and enabling sequence balancing on GRM 4G 1D and 110G 1D. We gradually scale the system from 8 GPUs to 64 GPUs. We report the gain values of sequence balancing at the top of figure.

cumulative training steps, detailing execution times for embedding lookup, forward, and backward phases. We can see that MTGRBoost achieves shorter execution times across all phases compared to TorchRec. The efficiency improvements derived from sequence balancing in dense model computations grow progressively more pronounced with increasing model complexity. Notably, expanding embedding table dimensions induces significant temporal increases in both lookup and backward phases, primarily stemming from embedding communication overhead and sparse parameter update latency. However, our implementation of automatic table merging and lookup deduplication substantially enhances execution efficiency in these critical phases.

6.3 Evaluation of Individual Designs

Ablation Study. Figure 13 presents an ablation study under 4G and 10G complexity settings by incrementally integrating different techniques in MTGRBoost. Starting with merging tables, we consolidate ID communication, embedding communication, and lookup operators from multiple feature tables into a single operation. Subsequently, a two-stage deduplication process is applied to feature IDs prior to embedding lookups. Finally, we introduce the sequence balancing strat-

Table 2: Batch sizes and average GPU memory utilization for three models with sequence balancing disabled versus enabled. Values before the arrow denotes fixed batch sizes with disabled state, while those after the arrow represent average ones over 1,000 steps with enabled state. Numbers in parentheses denote improvements in memory utilization.

Model	Batch size	GPU memory utilization
GRM 4G 1D	480 \rightarrow 496	86.3% \rightarrow 95.7% (+9.4)
GRM 110G 1D	80 \rightarrow 116	75.3% \rightarrow 90.3% (+15.0)

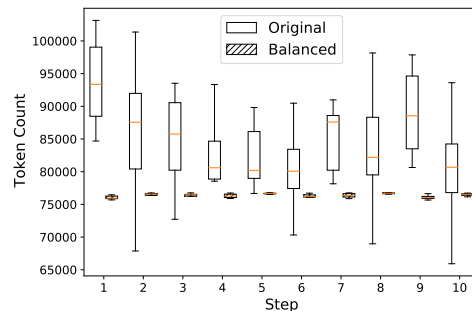


Figure 15: Original sequence vs. dynamic sequence batching. Each box denotes the minimum and maximum total token counts for GRM 4G 1D across 8 GPUs in one training step.

egy to optimize device load distribution, activating all MTGRBoost’s components.

The experimental results demonstrate consistent improvements across all proposed designs, indicating that every component in MTGRBoost is critical for enhancing overall system efficiency. Furthermore, we observe that performance gains intensify with higher computational complexity. This trend reveals a positive correlation between MTGRBoost’s efficiency improvements and computational complexity.

Sequence Balancing Evaluation. We further evaluate the proposed sequence balancing. We conduct experiments with GRM 4G and 110G. Starting with 8 GPUs, then we double the GPU count up to 64. To ensure fairness, batch sizes are adjusted to maintain near-full GPU utilization under both sequence balancing enabled and disabled conditions. Table 2 reports batch sizes and average GPU memory utilization, while Figure 14 presents throughput results with and without sequence balancing, yielding five key observations.

- Enabling sequence balancing in MTGRBoost achieves significant throughput improvements across all model variants and GPU configurations. Specifically, GRM 4G, and 110G exhibit average throughput improvements of 4.4%, and 26.5%, respectively, with GRM 110G on 64 GPUs showing a peak improvement of 33.5%.
- For a given model, throughput improvements scale with GPU count under sequence balancing. This is because that each step is constrained by the slowest device in syn-

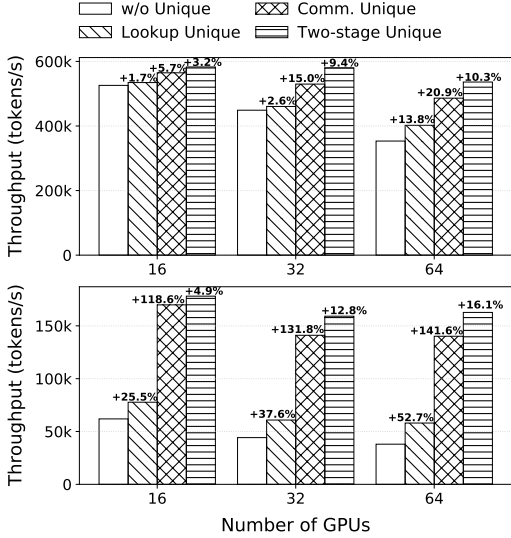


Figure 16: Throughput comparisons of two-stage ID deduplication for GRM 4G 1D (upper) and GRM 4G 64D (bottom). The improvements of the current strategy compared to the previous one are reported above the bars.

chronous training architectures. As the number of GPUs increases, the likelihood of encountering long sequences that induce computational delays rises.

- Throughput gains correlate positively with computational complexity. Since sequence processing FLOPs scale quadratically with token hidden dimensions, higher computational complexity amplifies load imbalance, which makes sequence balancing increasingly critical.
- Figure 15 illustrates reduced token count variance across GPUs after enabling sequence balancing, which stabilizes token counts at approximately 76,000 per device, effectively mitigating load imbalance.
- Table 2 shows that dynamic sequence batching can maximize GPU memory utilization via dynamic batch size regulation. In contrast, raw sequences would necessitate smaller batches to avoid out-of-memory errors from extreme sequence lengths, thereby degrading system efficiency.

The Effect of Two-stage ID Deduplication. To further evaluate the impact of two-stage ID deduplication on system efficiency, we fix the computational complexity at 4GFLOPs and conduct experiments with two embedding dimension factors of 1D and 64D. We employ four deduplication strategies: (a) *w/o unique* (i.e., no deduplication), (b) *Comm. unique* (i.e., first-stage deduplication only), (c) *Lookup unique* (i.e., second-stage deduplication only), and (d) *Two-stage unique* (i.e., both stages). Starting with 16 GPUs, we incrementally increase the GPU count and report throughput results in Figure 16. We get the following observations.

First, the two-stage approach achieves a $1.1\times$ – $3.7\times$ throughput improvement compared to the baseline (a), with

Table 3: Throughput comparison for MCH and MTGRBoost. OOM denotes out of memory and *Gain* denotes the throughput improvement. “-” indicates that the comparison cannot be made due to OOM problems.

Complexity	Dim. Factor	MCH	MTGRBoost	Gain
4G	1D	392,731	579,649	47.59%
	8D	260,590	438,190	68.2%
	64D	80,857	155,832	92.7%
110G	1D	44,719	68,993	54.28%
	8D	28,329	55,929	97.4%
	64D	OOM	38,575	-

gains amplifying at larger GPU scales. This finding highlights the effectiveness of two-stage deduplication in reducing ID communication, embedding communication, and lookup latency. Second, among single-stage strategies, “Comm. unique” outperforms “Lookup unique”. As embedding communication represents the primary latency source, whereas hash table lookups are inherently fast. Finally, deduplication benefits correlate with embedding dimensions: higher-dimensional embeddings amplify network bandwidth demands during cross-node transfers, which makes ID deduplication more important for reducing communication volume.

The Effect of Dynamic Embedding Table. To evaluate the effectiveness of the proposed dynamic embedding table in handling dynamic IDs, we conduct comparative experiments using Managed Collision Handling (MCH) as the baseline. MCH is designed by TorchRec to resolve changeable feature ID by maintaining a fixed-size mapping table to remap original IDs into a continuous space. It employs binary search for efficient ID localization and activates an eviction mechanism to update ID mappings when a threshold is reached.

Experimental results are shown in Table 3. Using a model with fixed computational complexity, we assess the throughput of both two techniques in handling embedding tables of varying scales by adjusting the embedding dimension factor. Our findings reveal that the dynamic embedding table achieves $1.47\times$ – $2.22\times$ throughput improvement than MCH. This improvement stems from the grouped parallel probing technique, which accelerates hash collision resolution via multi-threaded parallel probing. Furthermore, MCH encounters OOM issues at larger embedding dimensions due to pre-allocated memory for all tables. In contrast, the hash table requires substantially less initial memory and allocates additional resources only when thresholds are exceeded.

6.4 Scalability

We assess the system’s scalability by examining the deviation between actual speedup ratios and ideal linear scaling. Two factors are evaluated: computational complexity and embedding dimensions. (1) With the embedding dimension fixed

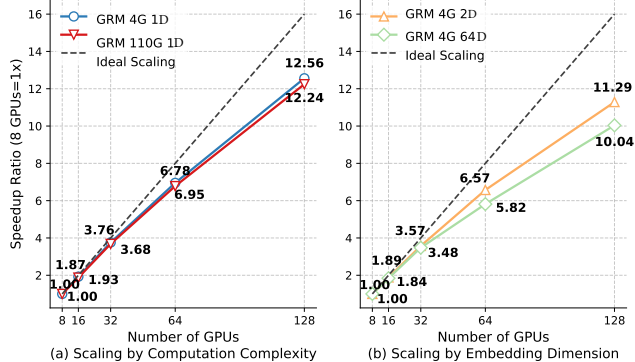


Figure 17: Comparison of scalability by (a) computational complexity and (b) embedding dimension. We use 1 node, 8 GPUs configuration as the baseline for speedup ratio. The specific speedup ratio values are marked near the broken line.

at 1D, we compare speedup ratios under computational complexities of 4G and 110G. (2) With computational complexity fixed at 4G, we compare speedup ratios for embedding dimensions of 2D and 64D. We use a 1 node, 8 GPUs configuration as the baseline and progressively scale to 16 nodes (in total 128 GPUs). Experimental results in Figure 17 reveal three key findings.

First, all systems exhibit sublinear scaling as GPU count increases, which attributes to communication overhead introduced by parallelism. However, MTGRBoost achieves 62.75%–78.5% of the ideal speedup ratio at 128 GPUs, which demonstrates its robust scalability. Second, scaling computational complexity by $27.5\times$ (GRM 4G 1D vs. 110G 1D) and embedding dimensions by $32\times$ (GRM 4G 2D vs. 4G 64D) results in minor speedup degradation. This stability arises from sequence balancing mitigating load imbalance under increased complexity, while merged tables and two-stage ID unique operation reduce lookup and communication latency. Third, embedding dimensions impact speedup more significantly than computational complexity. Since the latency of recommendation system is dominated by sparse embedding communication, computation, and updates, making scaling embedding dimensions more likely to affect performance.

7 Related Work

Systems for DRM training. Deep Recommendation Models (DRMs) combine sparse embeddings and dense neural networks to model each user-item individually. As DRMs are widely used, many systems are developed to accelerate its training [5–7, 13, 14, 18, 21, 23, 32, 38, 40, 46]. Specifically, Persia [21] decouples sparse embedding computation from dense model processing, training the embeddings asynchronously to improve throughput and the dense models synchronously to ensure accuracy. PICASSO [45] leverages the patterns of

model architecture and data distribution to accelerate execution with packing, interleaving, and caching optimizations. XDL [13] compresses the pair-wise communication among GPUs into a tree structure to accelerate embedding lookup and update. ScaleFreeCTR [7] leverages host memory to store massive embedding tables and employs GPU-optimized synchronization to update the embeddings. Zion [32] and RecSpeed [18] mitigate the I/O bottlenecks for embedding communication by deploying additional NICs. HugeCTR [38] tailors DRM training for NVIDIA DGX-1/DGX-2 platforms by optimizing embedding communication on NV-Switch interconnects. These systems are usually designed according to specific assumptions on the access patterns of the sparse embeddings (e.g., skewed towards the hot embeddings). We also plan to incorporate their optimizations after carefully analyzing the embedding access patterns in Meituan data. Moreover, their TensorFlow-based implementations require substantial efforts to migrate to PyTorch environments.

Systems for Transformer. To train Transformer efficiently, the focuses are attention computation and parallel strategies [3, 9, 12, 20, 22, 27–30, 35, 39]. FlashAttention [3] reduces the accesses to slow GPU global memory with tiled computation and online recomputation fusion. FlexFlow [22] and OptCNN [12] automatically search the optimal parallel strategy for model training by distributing model computation and parameters among the GPUs in different ways. GPipe [9] employs pipeline parallelism by splitting each mini-batches into micro-batches to interleave the computation and communication across the micro-batches. Megatron-LM [30] and DeepSpeed [28] propose hybrid parallel strategies for large-scale model training by partitioning the model and data across the GPUs. Hydraulis [20] adopts dynamic parallelism for each iteration according to the sequence length distribution to achieve workload balance. MTGRBoost enjoys existing attention kernel optimizations for efficient computation but simple data parallel suffices for GRMs since their dense models are usually small. Moreover, MTGRBoost optimizes the processing of sparse embeddings, which are not present in most Transformer-based models.

8 Conclusion

In this paper, we propose MTGRBoost, a distributed training system addressing scalability and efficiency challenges in industrial generative recommendation models (GRMs). For sparse model, we introduce dynamic embedding tables for changeable feature IDs, automated table merging and two-stage ID deduplication for embedding optimizations. For dense model, dynamic sequence balancing alleviates the workload imbalances. A suite of other techniques are integrated to ensure system availability. Experimental results demonstrate substantial improvements in training efficiency while maintaining model accuracy. MTGRBoost provides a flexible and

efficient solution for industrial applications, paving the way for broader adoption of GRM in recommendation systems.

References

- [1] Josh Achiam, Steven Adler, Sandhini Agarwal, Lama Ahmad, Ilge Akkaya, Florencia Leoni Aleman, Diogo Almeida, Janko Altenschmidt, Sam Altman, Shyamal Anadkat, et al. Gpt-4 technical report. *arXiv preprint arXiv:2303.08774*, 2023.
- [2] Austin Appleby. Murmurhash. <https://github.com/aappleby/smhasher>, 2008. Accessed: 2023-10-15.
- [3] Tri Dao, Dan Fu, Stefano Ermon, Atri Rudra, and Christopher Ré. Flashattention: Fast and memory-efficient exact attention with io-awareness. *Advances in neural information processing systems*, 35:16344–16359, 2022.
- [4] Jiaxin Deng, Shiyao Wang, Kuo Cai, Lejian Ren, Qigen Hu, Weifeng Ding, Qiang Luo, and Guorui Zhou. Onerec: Unifying retrieve and rank with generative recommender and iterative preference alignment. *arXiv preprint arXiv:2502.18965*, 2025.
- [5] Miao Fan, Jiacheng Guo, Shuai Zhu, Shuo Miao, Mingming Sun, and Ping Li. Mobius: Towards the next generation of query-ad matching in baidu’s sponsored search. In *Proceedings of the 25th ACM SIGKDD international conference on knowledge discovery and data mining*, pages 2509–2517, 2019.
- [6] Yufei Feng, Binbin Hu, Fuyu Lv, Qingwen Liu, Zhiqiang Zhang, and Wenwu Ou. Atbrg: Adaptive target-behavior relational graph network for effective recommendation. In *Proceedings of the 43rd international ACM SIGIR conference on research and development in information retrieval*, pages 2231–2240, 2020.
- [7] Huifeng Guo, Wei Guo, Yong Gao, Ruiming Tang, Xiquang He, and Wenzhi Liu. Scalefreectr: Mixcache-based distributed training system for ctr models with huge embedding table. In *Proceedings of the 44th international ACM SIGIR conference on research and development in information retrieval*, pages 1269–1278, 2021.
- [8] Lei Huang, Hao Guo, Linzhi Peng, Long Zhang, Xiaoteng Wang, Daoyuan Wang, Shichao Wang, Jinpeng Wang, Lei Wang, and Sheng Chen. Sessionrec: Next session prediction paradigm for generative sequential recommendation. *arXiv preprint arXiv:2502.10157*, 2025.
- [9] Yanping Huang, Youlong Cheng, Ankur Bapna, Orhan Firat, Dehao Chen, Mia Chen, HyoukJoong Lee, Jiquan Ngiam, Quoc V Le, Yonghui Wu, et al. Gpipe: Efficient training of giant neural networks using pipeline parallelism. *Advances in neural information processing systems*, 32, 2019.
- [10] Dmytro Ivchenko, Dennis Van Der Staay, Colin Taylor, Xing Liu, Will Feng, Rahul Kindi, Anirudh Sudarshan, and Shahin Sefati. Torchrec: a pytorch domain library for recommendation systems. In *Proceedings of the 16th ACM conference on recommender systems*, pages 482–483, 2022.
- [11] Jianchao Ji, Zelong Li, Shuyuan Xu, Wenyue Hua, Yingqiang Ge, Juntao Tan, and Yongfeng Zhang. Genrec: Large language model for generative recommendation. In *European conference on information retrieval*, pages 494–502. Springer, 2024.
- [12] Zhihao Jia, Sina Lin, Charles R Qi, and Alex Aiken. Exploring hidden dimensions in parallelizing convolutional neural networks. In *Proceedings of the international conference on machine learning*, volume 2279, page 2288, 2018.
- [13] Biye Jiang, Chao Deng, Huimin Yi, Zelin Hu, Guorui Zhou, Yang Zheng, Sui Huang, Xinyang Guo, Dongyue Wang, Yue Song, et al. Xdl: an industrial deep learning framework for high-dimensional sparse data. In *Proceedings of the 1st international workshop on deep learning practice for high-dimensional sparse data*, pages 1–9, 2019.
- [14] Peng Jiang and Gagan Agrawal. A linear speedup analysis of distributed deep learning with sparse and quantized communication. *Advances in neural information processing systems*, 31, 2018.
- [15] Nikhil Ketkar, Jojo Moolayil, Nikhil Ketkar, and Jojo Moolayil. Introduction to pytorch. *Deep learning with python: learn best practices of deep learning models with PyTorch*, pages 27–91, 2021.
- [16] Diederik P Kingma and Jimmy Ba. Adam: A method for stochastic optimization. *arXiv preprint arXiv:1412.6980*, 2014.
- [17] Mario Michael Krell, Matej Kosec, Sergio P Perez, and Andrew Fitzgibbon. Efficient sequence packing without cross-contamination: Accelerating large language models without impacting performance. *arXiv preprint arXiv:2107.02027*, 2021.
- [18] Suresh Krishna and Ravi Krishna. Accelerating recommender systems via hardware" scale-in". *arXiv preprint arXiv:2009.05230*, 2020.

- [19] Achintya Kundu, Rhui Dih Lee, Laura Wynter, Raghu Kiran Ganti, and Mayank Mishra. Enhancing training efficiency using packing with flash attention. *arXiv preprint arXiv:2407.09105*, 2024.
- [20] Haoyang Li, Fangcheng Fu, Sheng Lin, Hao Ge, Xuanyu Wang, Jiawen Niu, Jie Jiang, and Bin Cui. Demystifying workload imbalances in large transformer model training over variable-length sequences. *arXiv preprint arXiv:2412.07894*, 2024.
- [21] Xiangru Lian, Binhang Yuan, Xuefeng Zhu, Yulong Wang, Yongjun He, Honghuan Wu, Lei Sun, Haodong Lyu, Chengjun Liu, Xing Dong, et al. Persia: An open, hybrid system scaling deep learning-based recommenders up to 100 trillion parameters. In *Proceedings of the 28th ACM SIGKDD conference on knowledge discovery and data mining*, pages 3288–3298, 2022.
- [22] Wenyan Lu, Guihai Yan, Jiajun Li, Shijun Gong, Yinhe Han, and Xiaowei Li. Flexflow: A flexible dataflow accelerator architecture for convolutional neural networks. In *2017 IEEE international symposium on high performance computer architecture (HPCA)*, pages 553–564. IEEE, 2017.
- [23] Xupeng Miao, Hailin Zhang, Yining Shi, Xiaonan Nie, Zhi Yang, Yangyu Tao, and Bin Cui. Het: Scaling out huge embedding model training via cache-enabled distributed framework. *arXiv preprint arXiv:2112.07221*, 2021.
- [24] Deepak Narayanan, Aaron Harlap, Amar Phanishayee, Vivek Seshadri, Nikhil R Devanur, Gregory R Ganger, Phillip B Gibbons, and Matei Zaharia. Pipedream: Generalized pipeline parallelism for dnn training. In *Proceedings of the 27th ACM symposium on operating systems principles*, pages 1–15, 2019.
- [25] Maxim Naumov, Dheevatsa Mudigere, Hao-Jun Michael Shi, Jianyu Huang, Narayanan Sundaraman, Jongsoo Park, Xiaodong Wang, Udit Gupta, Carole-Jean Wu, Alisson G Azzolini, et al. Deep learning recommendation model for personalization and recommendation systems. *arXiv preprint arXiv:1906.00091*, 2019.
- [26] Alec Radford, Karthik Narasimhan, Tim Salimans, Ilya Sutskever, et al. Improving language understanding by generative pre-training. 2018.
- [27] Samyam Rajbhandari, Jeff Rasley, Olatunji Ruwase, and Yuxiong He. Zero: Memory optimizations toward training trillion parameter models. In *International conference for high performance computing, networking, storage and analysis*, pages 1–16. IEEE, 2020.
- [28] Jeff Rasley, Samyam Rajbhandari, Olatunji Ruwase, and Yuxiong He. Deepspeed: System optimizations enable training deep learning models with over 100 billion parameters. In *Proceedings of the 26th ACM SIGKDD international conference on knowledge discovery and data mining*, pages 3505–3506, 2020.
- [29] Jie Ren, Samyam Rajbhandari, Reza Yazdani Aminabadi, Olatunji Ruwase, Shuangyan Yang, Minjia Zhang, Dong Li, and Yuxiong He. {Zero-offload}: Democratizing {billion-scale} model training. In *2021 USENIX annual technical conference*, pages 551–564, 2021.
- [30] Mohammad Shoeybi, Mostofa Patwary, Raul Puri, Patrick LeGresley, Jared Casper, and Bryan Catanzaro. Megatron-lm: Training multi-billion parameter language models using model parallelism. *arXiv preprint arXiv:1909.08053*, 2019.
- [31] Pramod Singh, Avinash Manure, Pramod Singh, and Avinash Manure. Introduction to tensorflow 2.0. *Learn TensorFlow 2.0: implement machine learning and deep learning models with python*, pages 1–24, 2020.
- [32] Misha Smelyanskiy. Zion: Facebook next-generation large memory training platform. In *2019 31th IEEE hot chips symposium*, pages 1–22. IEEE, 2019.
- [33] Hugo Touvron, Thibaut Lavril, Gautier Izacard, Xavier Martinet, Marie-Anne Lachaux, Timothée Lacroix, Baptiste Rozière, Naman Goyal, Eric Hambro, Faisal Azhar, et al. Llama: Open and efficient foundation language models. *arXiv preprint arXiv:2302.13971*, 2023.
- [34] Ashish Vaswani, Noam Shazeer, Niki Parmar, Jakob Uszkoreit, Llion Jones, Aidan N Gomez, Łukasz Kaiser, and Illia Polosukhin. Attention is all you need. *Advances in neural information processing systems*, 30, 2017.
- [35] Guanhua Wang, Heyang Qin, Sam Ade Jacobs, Connor Holmes, Samyam Rajbhandari, Olatunji Ruwase, Feng Yan, Lei Yang, and Yuxiong He. Zero++: Extremely efficient collective communication for giant model training. *arXiv preprint arXiv:2306.10209*, 2023.
- [36] Ruoxi Wang, Bin Fu, Gang Fu, and Mingliang Wang. Deep & cross network for ad click predictions. In *Proceedings of the ADKDD'17*, pages 1–7. 2017.
- [37] Wenjie Wang, Xinyu Lin, Fuli Feng, Xiangnan He, and Tat-Seng Chua. Generative recommendation: Towards next-generation recommender paradigm. *arXiv preprint arXiv:2304.03516*, 2023.
- [38] Zehuan Wang, Yingcan Wei, Minseok Lee, Matthias Langer, Fan Yu, Jie Liu, Shijie Liu, Daniel G Abel,

- Xu Guo, Jianbing Dong, et al. Merlin hugectr: Gpu-accelerated recommender system training and inference. In *Proceedings of the 16th ACM conference on recommender systems*, pages 534–537, 2022.
- [39] Houming Wu, Ling Chen, and Wenjie Yu. Bitpipe: Bidirectional interleaved pipeline parallelism for accelerating large models training. *arXiv preprint arXiv:2410.19367*, 2024.
- [40] Minhui Xie, Kai Ren, Youyou Lu, Guangxu Yang, Qingxing Xu, Bihai Wu, Jiazhen Lin, Hongbo Ao, Wanhong Xu, and Jiwu Shu. Kraken: Memory-efficient continual learning for large-scale real-time recommendations. In *SC20: International conference for high performance computing, networking, storage and analysis*, pages 1–17. IEEE, 2020.
- [41] Jun Xu, Xiangnan He, and Hang Li. Deep learning for matching in search and recommendation. In *The 41st International ACM SIGIR conference on research and development in information retrieval*, pages 1365–1368, 2018.
- [42] Songpei Xu, Shijia Wang, Da Guo, Xianwen Guo, Qiang Xiao, Fangjian Li, and Chuanjiang Luo. An efficient large recommendation model: Towards a resource-optimal scaling law. *arXiv preprint arXiv:2502.09888*, 2025.
- [43] Bencheng Yan, Shilei Liu, Zhiyuan Zeng, Zihao Wang, Yizhen Zhang, Yujin Yuan, Langming Liu, Jiaqi Liu, Di Wang, Wenbo Su, et al. Unlocking scaling law in industrial recommendation systems with a three-step paradigm based large user model. *arXiv preprint arXiv:2502.08309*, 2025.
- [44] Jiaqi Zhai, Lucy Liao, Xing Liu, Yueming Wang, Rui Li, Xuan Cao, Leon Gao, Zhaojie Gong, Fangda Gu, Michael He, et al. Actions speak louder than words: Trillion-parameter sequential transducers for generative recommendations. *arXiv preprint arXiv:2402.17152*, 2024.
- [45] Yuanxing Zhang, Langshi Chen, Siran Yang, Man Yuan, Huimin Yi, Jie Zhang, Jiamang Wang, Jianbo Dong, Yunlong Xu, Yue Song, et al. Picasso: Unleashing the potential of gpu-centric training for wide-and-deep recommender systems. In *2022 IEEE 38th international conference on data engineering*, pages 3453–3466. IEEE, 2022.
- [46] Weijie Zhao, Deping Xie, Ronglai Jia, Yulei Qian, Ruiquan Ding, Mingming Sun, and Ping Li. Distributed hierarchical gpu parameter server for massive scale deep learning ads systems. *Proceedings of machine learning and systems*, 2:412–428, 2020.
- [47] Guorui Zhou, Xiaoqiang Zhu, Chenru Song, Ying Fan, Han Zhu, Xiao Ma, Yanghui Yan, Junqi Jin, Han Li, and Kun Gai. Deep interest network for click-through rate prediction. In *Proceedings of the 24th ACM SIGKDD international conference on knowledge discovery and data mining*, pages 1059–1068, 2018.

A Proof

We use coprime conditions and the characteristics of moduli to prove that our grouped parallel probing technique can traverse all slots in the hash table.

Lemma 1 *If $M = 2^n$ and S is odd, then $\gcd(S, M) = 1$. \gcd denotes the greatest common divisor.*

Proof 1 *S contains no factor of 2 (since S is odd), while M has prime factorization 2^n . Thus, S and M share no common prime factors, proving $\gcd(S, M) = 1$.*

Proof 2 *Assume there exist $t_1, t_2 \in [0, M-1]$, $t_1 \neq t_2$ such that:*

$$h_{t_1} \equiv h_{t_2}, \quad (9)$$

This implies:

$$(t_1 - t_2) \cdot S \equiv 0. \quad (10)$$

By Lemma 1, $\gcd(S, M) = 1$. According to Bézout’s identity, S has a multiplicative inverse modulo M . Multiplying both sides by this inverse yields:

$$t_1 - t_2 \equiv 0. \quad (11)$$

Since $t_1, t_2 \in [0, M-1]$, the only solution is $t_1 = t_2$, contradicting the initial assumption. Hence, all probe positions are unique.

Proof 3 *By the pigeonhole principle, M probes generate M unique positions, exactly covering all slots:*

$$\{h_t\}_{t=0}^{M-1} = \{0, 1, 2, \dots, M-1\}. \quad (12)$$